Experimental evidence of deterministic coherence resonance in coupled chaotic systems with frequency mismatch

M. A. García-Vellisca,[1] A. N. Pisarchik,[1,2,*] and R. Jaimes-Reátegui[1,3]

[1]*Center for Biomedical Technology, Technical University of Madrid, Campus Montegancedo, 28223 Pozuelo de Alarcon, Madrid, Spain*
[2]*Centro de Investigaciones en Optica, Loma del Bosque 115, 37150 Leon, Guanajuato, Mexico*
[3]*Centro Universitario de los Lagos, Universidad de Guadalajara, Enrique Díaz de Leon, Paseos de la Montaña, Lagos de Moreno, Jalisco 47460, Mexico*

We present the experimental evidence of deterministic coherence resonance in unidirectionally coupled two and three Rössler electronic oscillators with mismatch between their natural frequencies. The regularity in both the amplitude and the phase of chaotic fluctuations is experimentally proven by the analyses of normalized standard deviations of the peak amplitude and interpeak interval and Lyapunov exponents. The resonant chaos suppression appears when the coupling strength is increased and the oscillators are in phase synchronization. In two coupled oscillators, the coherence enhancement is associated with negative third and fourth Lyapunov exponents, while the largest first and second exponents remain positive. Distinctly, in three oscillators coupled in a ring, all exponents become negative, giving rise to periodicity. Numerical simulations are in good agreement with the experiments.

I. INTRODUCTION

Chaos is an important form of dynamical movement in nature. The emergence of order from chaos is one of the greatest mysteries of the universe. Ilya Prigogine, a Belgian scientist who received a Nobel Prize in 1977 for his work on thermodynamics of systems operating dynamically under nonequilibrium conditions, argued that systems far from equilibrium, with a high flow-through of energy, could produce a higher degree of order. In his famous book "Order Out of Chaos" [1], he wrote that in conditions far from equilibrium, we may have transformation from disorder (thermal chaos) into order. However, since all of his Nobel-Prize winning discussions have been philosophical and mathematical (not experimental), some scientists criticized his view of evolution from chaos to order, saying that such phenomena may be manipulated on paper or on a computer screen but not in real life. The experimental manifestation of the emergence of periodicity in interacting chaotic systems may shed light on the understanding of essential mechanisms leading to self-organization of matter.

In the late 20th century, when the computational techniques became an important scientific tool, many scientists focused their efforts on developing deterministic methods to stabilize chaos. Since a chaotic attractor is composed by an infinite number of unstable periodic orbits, several researchers proposed to stabilize an unstable periodic orbit embedded within the chaotic attractor using feedback and nonfeedback control methods (for comprehensive review see Refs. [2,3] and references therein). The most recognized techniques of feedback control, the Ott, Grebogi and Yorke (OGY) [4] and Pyragas [5] methods, are based on an adjustment of, respectively, a system parameter or a variable. Since these methods require a very small change in the parameter or variable, the control is assumed to be small. Instead,

nonfeedback control requires an external modulation to induce a new stable orbit [6–10] and therefore cannot be considered small, because the external forcing should be strong enough to modify the system dynamics.

The regularity or coherence of a chaotic system can also be improved by noise. Sometimes, the influence of noise has a resonance character referred to as noise-induced coherence resonance. This effect was detected in both excitable [11–16] and bistable [17–19] systems. Later, a similar behavior was discovered in completely deterministic systems without any noise. For example, in a bistable system chaos plays a role similar to noise by inducing switches between coexisting states; the switches become more regular at a certain amplitude of the chaotic signal [20–22]. Such an effect, known as *deterministic coherence resonance*, was also observed in monostable chaotic systems subject to time-delayed feedback [23–26], where the increasing feedback signal induced optimal regularity in the chaotic system.

On the other hand, dynamics of a chaotic system can be regularized due to its interaction with other systems in order to reach a synchronous state. In fact, synchronization is an example of self-organization in nature [27,28], and it is usually assumed that the interaction between oscillators enhances their synchronization. However, this is not always true. Indeed, the increasing coupling between chaotic systems may result in unexpected behaviors, such as, e.g., oscillation death [29,30] and coherence enhancement [31,32]. The latter was predicted only theoretically in two coupled oscillators. It was surprisingly found [32] that adequate coupling can force a chaotic oscillator towards more regular oscillations, so although coupled oscillators have the same dominant frequency in their power spectra, they follow different phase trajectories. In terms of synchronization theory, this means that the oscillators are phase synchronized [33], i.e., they develop a perfect phase-locking relation for relatively weak coupling although their amplitudes remain almost uncorrelated [34–37]. Chaos suppression in coupled chaotic oscillators was found in two cases, first, in the presence of asymmetry in coupling

———————
*alexander.pisarchik@ctb.upm.es

and, second, when there is a small mismatch between natural frequencies of the coupled oscillators. While the former was observed in bidirectionally coupled identical systems [31], the latter was theoretically predicted in unidirectionally coupled oscillators [32].

Phase synchronization is abundant in science and plays a crucial role in many weakly interacting natural systems, including lasers [38], electronic circuits [39–41], cardiorespiratory rhythm [42], neurons [43,44], behavioral psychology [45], and ecology [46,47]. Although synchronization of unidirectionally coupled chaotic oscillators has been extensively investigated [33], some features are not yet well understood, in particular, in the presence of a small detuning between natural frequencies of the coupled oscillators. Recently, we have shown [32] that a chaotic slave oscillator coupled with a chaotic master oscillator becomes more regular when the oscillators are in phase synchronization. We have found that such coherence enhancement has a resonant character with respect to both the coupling strength and frequency mismatch. The main aim of the present work is to provide the experimental evidence for this resonance phenomenon. Since the experimental parameters do not coincide with the numerical parameters used in Ref. [32], we will perform numerical simulations of the same equations, but with parameters exactly matched the experimental ones, and compare the obtained experimental and numerical results. Furthermore, to demonstrate the generality of the deterministic coherence resonance, we will also consider another coupling scheme, namely a ring of unidirectionally coupled chaotic oscillators.

A system of coupled oscillators can be described as $\dot{\mathbf{x}}_j = \mathbf{F}(\mathbf{x}_j, \omega_j) + \sigma_{ji}(\mathbf{x}_i - \mathbf{x}_j)$, where $\mathbf{x}_{j,i}$ are vectors of state variables of jth and ith oscillators, $\mathbf{F}$ is a vector function, and σ_{ji} is a coupling strength. The oscillators are only distinct by their natural frequencies ($\omega_j \neq \omega_i$). Due to nonlinearity, the dominant frequency Ω_j in the chaotic power spectrum of the uncoupled jth oscillator usually does not coincide with its natural frequency ($\Omega_j \neq \omega_j$). When the oscillators are unidirectionally coupled, the ith oscillator drives the jth oscillator. Thus, the former acts as a master, while the latter acts as a slave. For sufficiently strong coupling, the master oscillator i entrains the dominant frequency Ω_j of the slave oscillator j, which results in phase synchronization [35]. The time-averaged difference between the oscillators' phases $\delta_{ji} = \langle \varphi_j - \varphi_i \rangle$ is negative ($\delta_{ji} < 0$) if the frequency mismatch $\Delta_{ji} = \omega_j - \omega_i < 0$ and positive ($\delta_{ji} > 0$) if $\Delta_{ji} > 0$. In the former case, the phase of the slave oscillator is locked by the master oscillator with lag, whereas in the latter case with anticipation [48].

Deterministic coherence resonance in two unidirectionally coupled Rössler oscillators with small mismatch between their natural frequencies has been theoretically described in Ref. [32]. In the regime of phase synchronization, the coherence of the slave oscillator was shown to reach the maximum with respect to both the frequency mismatch Δ_{ji} and the coupling strength σ_{ji}. This coherence enhancement was attributed to the third and fourth Lyapunov exponents which took negative values in the parameter range where the resonance was observed. Here, we present the experimental evidence of this surprising phenomenon in two and three unidirectionally coupled oscillators. This effect resembles

"stabilization of chaos by chaos," i.e., the chaotic system at a certain coupling strength and a frequency mismatch behaves more regularly in two coupled oscillators and completely periodically in a ring of three oscillators.

The rest of the paper is organized as follows. In Sec. II we describe the model and present experimental results demonstrating deterministic coherence resonance in two and three coupled Rössler electronic circuits. In Sec. III we discuss the results of numerical simulations and compare them with the experiments. The main conclusions are given in Sec. IV.

II. EXPERIMENT

A. Experimental setup

The experimental setup is constructed on the base of the electronic circuits shown in Fig. 2. These circuits are analog implementations of the Rössler oscillator [49] and the diffusive coupling.

The Kirchhoff's mesh analysis yields the following equations:

$$\begin{aligned}
\dot{V}_{xj} &= -\alpha A(V_{yj} + V_{zj}), \\
\dot{V}_{yj} &= \alpha[B V_{xj} + C V_{yj} + \sigma_{ji}(V_{yi} - V_{yj})], \qquad (1) \\
\dot{V}_{zj} &= \alpha[D + E V_{zj}(V_{xj} - F)],
\end{aligned}$$

where V_{xj}, V_{yj}, and V_{zj} are the output voltages of the three meshes, $\alpha = 10^3$ s^{-1} is the time scale coefficient, σ_{ji} is the coupling strength between the oscillators j and i defined by the parameters of the coupler [Fig. 1(b)], and A, B, C, D, E, and F are the parameters expressed in terms of electronic
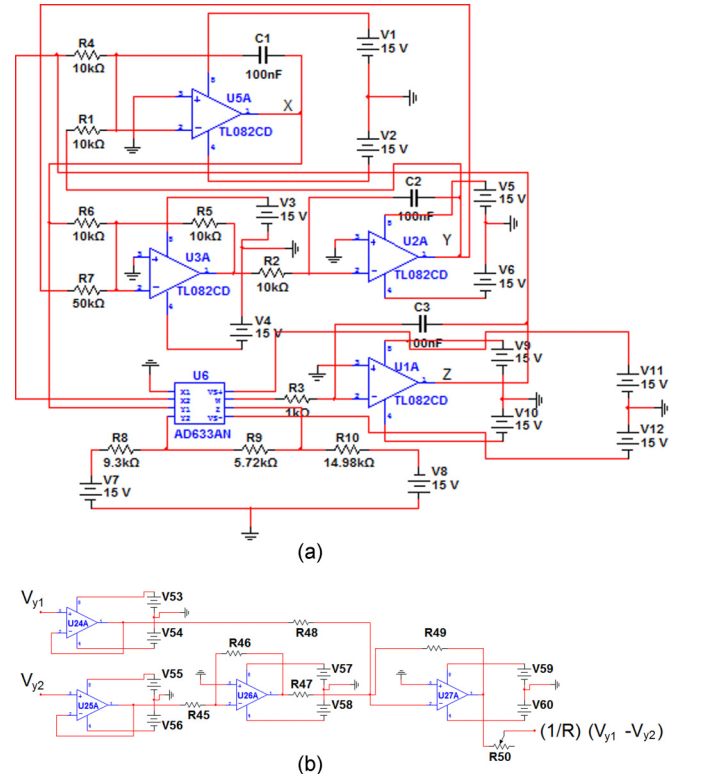

FIG. 1. Electronic schemes of (a) Rössler oscillator and (b) coupler.

components as

$$A = C_1 R_1, B = \frac{R_5}{C_1 R_2 R_6} = 1, \quad C = \frac{R_5}{C_1 R_2 R_7},$$

$$D = \frac{V_0}{10 C_3 R_3}\left(\frac{1 - 2R_{10}}{R_8 + R_9 + R_{10}}\right), \quad E = \frac{15}{V_0} = 1, \quad (2)$$

$$F = \frac{V_0}{10 C_3 R_3}\left(1 - \frac{2R_8}{R_8 + R_9 + R_{10}}\right),$$

where $V_0 = 15$ V is the power voltage of each mesh.

Although in Eq. (1) the coupling is realized through variable V_y, our experiments show that there is no principal difference if the oscillators are coupled through variable V_x. Since we observe coherence resonance in both cases, here we will only present the results for the coupling given by Eq. (1).

We carry out two kinds of experiments. First, we study two unidirectionally coupled Rössler oscillators and, second, three oscillators unidirectionally coupled in a ring. The natural frequencies of the oscillators are determined by resistors R1 and R6, different for every oscillator. Since these resistors are not variable, in the experiments we do not use the natural frequencies as control parameters because variable resistors with the required variation step are not available. The full experimental process is controlled with a virtual interface developed in LABVIEW 8.5, which can be considered as a state machine. The coupling strength is regulated by variable resistor $R_{50} = 3/300$ kΩ with a step of 3 kΩ. Since $\sigma_{ji} \sim 1/R_{50}$, the oscillators can be considered to be uncoupled when R_{50} is high ($R_{50} = 300$ kΩ). This weak coupling does not act as a residual noise source able to synchronize the oscillators phases.

The experimental procedure is realized as follows. First, the coupling is set to the minimum value ($R_{50} = 300$ kΩ). After a waiting time of 500 ms (roughly corresponding to 60 cycles of the autonomous system), the output signals from all circuits are acquired by analog ports. Once the dynamics of the whole system is recorded, the value of R_{50} is decreased by one step (3 kΩ), and the signals are again stored in the PC for further analysis. This process is repeated until the maximum coupling ($R_{50} = 3$ kΩ) is reached.

B. Two coupled oscillators

The parameters of two Rössler oscillators in the master-slave configuration (master $i = 1$, slave $j = 2$) are chosen so when uncoupled both oscillators are in a chaotic regime. Since the coupling is unidirectional, we set $\sigma_{12} = 0$ and $\sigma_{21} = \sigma$. We observe that at a certain coupling the slave oscillator becomes more coherent. A glimpse of the results are present in Fig. 2 with the time series [Figs. 2(a) and 2b)], power spectra [Figs. 2(c) and 2d)], and phase-space trajectories [Figs. 2(e) and 2f)] of the uncoupled and coupled oscillators. As seen in Fig. 2(f), the attractor of the slave oscillator shrinks, meaning that the oscillations become more regular.

The resistors R1 and R6 in the master and slave electronic circuits are chosen so the dominant frequencies of the uncoupled oscillators are, respectively, $f_1 = 162$ Hz and $f_2 = 191$ Hz [Fig. 2(e)]. With sufficiently strong coupling the oscillators' phases become synchronized [Fig. 2(b)] because the master oscillator entrains the dominant frequency of the
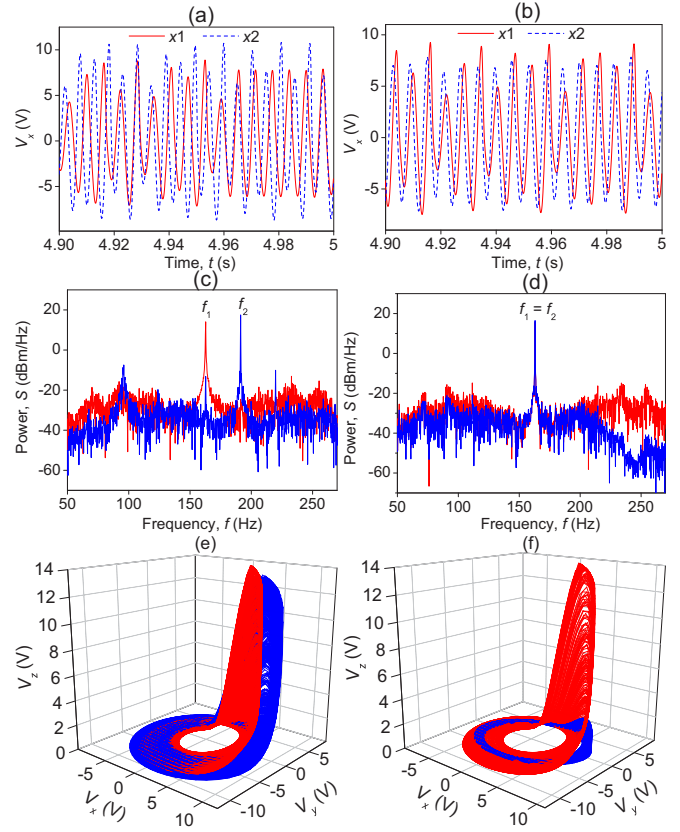

FIG. 2. Experimental [(a) and (b)] time series, [(c) and (d)] power spectra, and [(e) and (f)] attractors of uncoupled (left-hand column) and coupled oscillators with coupling $1/R_{50} = 2 \times 10^{-5}$ (right-hand column). f_1 and f_2 are the dominant frequencies in the power spectra. The coherence enhancement in the slave oscillator is characterized by the shrinking of the attractor (dark blue line) in the phase space.

slave oscillator, so the oscillators have the same dominant frequency in their power spectra [Fig. 2(d)]. This coupling leads to chaos suppression in the slave oscillator clearly seen in the phase-space plot in Fig. 2(f).

For quantitative description of coherence, we use (i) the peak value of the variable V_{y2}, (ii) interpeak intervals (IPI), (iii) normalized standard deviation (NSD) of the peak value of V_{y2}, and (iv) NSD of IPI. In Fig. 3 we plot all these characteristics for variable V_{y2} as a function of the coupling strength.

The minimum of NSD in Fig. 3(c) is the signature of amplitude coherence, while the minimum of NSD in Fig. 3(d) indicates time coherence. Interestingly, the coherence in time and amplitude occur for distinct coupling strengths.

The video of recorded oscilloscope traces shown in the Supplemental Material [50] demonstrates the emergence of coherence resonance in two coupled electronic circuits while the coupling strength is increasing.

C. Three coupled oscillators

Now we consider a ring of three unidirectionally coupled chaotic Rössler oscillators. In this configuration, each oscillator acts simultaneously as a master for one oscillator and a slave for another. All oscillators are coupled with the same coupling strength $\sigma_{21} = \sigma_{32} = \sigma_{13} = \sigma$. Since the coupling
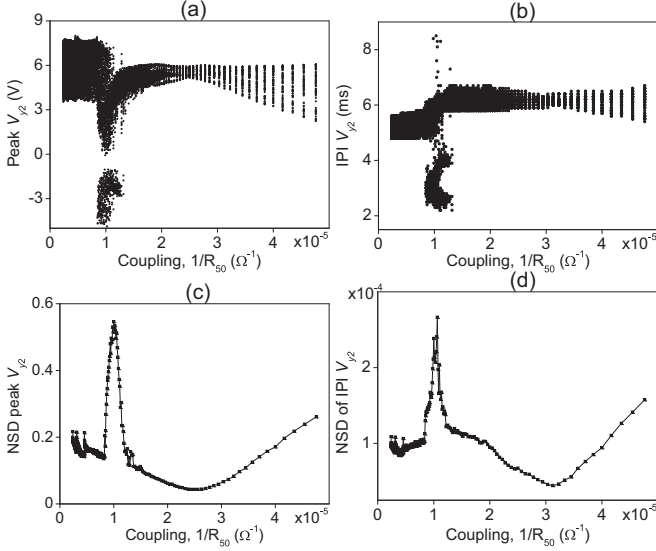
FIG. 3. Experimental (a) peak value of V_{y2}, (b) interpeak intervals (IPI), (c) normalized standard deviation (NSD) of peak value, and (d) NSD of IPI versus coupling strength.

is unidirectional, $\sigma_{12} = \sigma_{23} = \sigma_{31} = 0$. The resistors R1 and R6 in each of the three circuits are chosen so the dominant frequencies in the chaotic power spectra of the uncoupled oscillators are in an ascending order, i.e., $f_1 < f_2 < f_3$, where $f_1 = 152$ Hz, $f_2 = 168$ Hz, and $f_3 = 177$ Hz. The time series, phase portraits, and power spectra of the uncoupled and coupled oscillators are shown in Fig. 4. For sufficiently strong coupling, the oscillators in phase synchronization [Fig. 4(b)] have the same dominant frequency $f_c = 170$ Hz [Fig. 4(d)], close to the dominant frequency of the oscillator with the highest energy (in our case this is the oscillator 3). While the uncoupled or weakly coupled oscillators are chaotic [Figs. 4(a) and 4(c)], for an intermediate coupling strength they behave completely periodically [Figs. 4(b) and 4(d)]. The small local
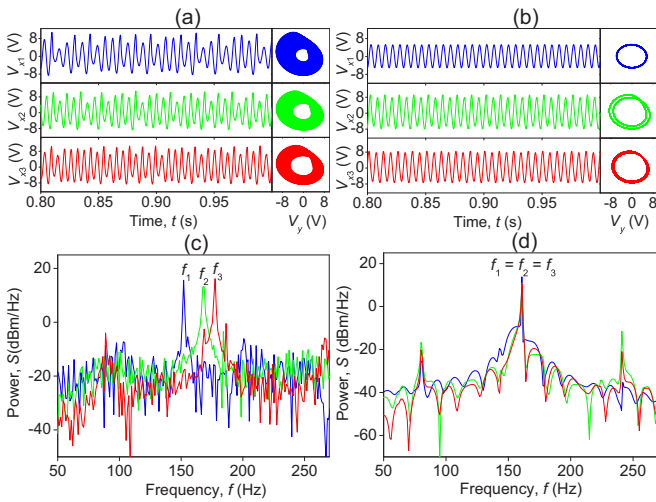

FIG. 4. Experimental [(a) and (b)] time series, phase portraits, and [(c) and (d)] power spectra of three [(a) and (c)] uncoupled and [(b) and (d)] coupled Rössler oscillators demonstrating coherence enhancement for $1/R_{50} \approx 2 \times 10^{-5}$ Ω^{-1}.
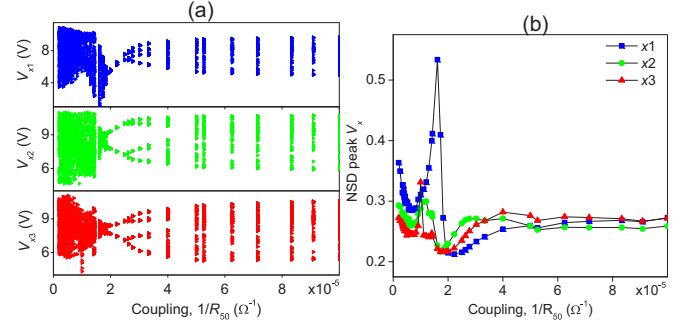

FIG. 5. Experimental (a) peak output voltages of three oscillators and (b) normalized standard deviations of peak voltages as a function of the coupling strength demonstrating coherence resonance for $1/R_{50} \approx 2 \times 10^{-5}$ Ω^{-1}.

maxima in the power spectra at $f \approx 88$ Hz indicate that the oscillators are in the period-2 regime.

When the coupling strength is further increased, the oscillators become chaotic again. The coherence resonance is clearly seen in the bifurcation diagrams of the peak voltages [Fig. 5(a)] and NSD of these peaks [Fig. 5(b)].

III. NUMERICAL SIMULATIONS

We perform numerical simulations of the following system of equations:

$$\dot{x}_j = -\omega_j y_j - z_j,$$
$$\dot{y}_j = \omega_j x_j + a y_j + \sigma_{ji}(y_i - y_j), \qquad (3)$$
$$\dot{z}_j = b + z_j(x_j - c),$$

where x_j, y_j, and z_j are the state variables of the jth oscillator. The system Eq. (3) is the dimensionless model of the experimental system Eq. (1). To simulate our experiments numerically, we consider the same configurations as in the experiments, i.e., two and three coupled oscillators. While in the experiments the oscillators' natural frequencies ω_j were not varied due to technical difficulties, in the numerical simulations we used frequency mismatch $\Delta_{ji} = \omega_j - \omega_i$ as a control parameter, in addition to the coupling strength $\sigma_{ji} = \sigma$.

A. Two coupled oscillators

In the numerical simulations we use the same parameters as in the experiment, namely $a = \alpha C = 0.2$, $b = \alpha D = 0.2$, and $c = \alpha F = 5.7$. The natural frequency of the master oscillator is fixed to $\omega_1 = 1$ to provide a chaotic regime.

Figure 6 illustrates how mismatch $\Delta \equiv \Delta_{21} = \omega_2 - \omega_1 = 0.1$ between the natural frequencies of the slave and master oscillators enhances coherence of the slave oscillator dynamics.

The uncoupled oscillators are chaotic [Figs. 6(a), 6(c), and 6(e)] with different dominant frequencies in their power spectra, $\Omega_1 = 1.07$ and $\Omega_2 = 1.16$ [Fig. 6(c)]. Due to nonlinearity, they are shifted with respect to the natural frequencies $\omega_1 = 1$ and $\omega_2 = 1.1$. When the oscillators are coupled with $\sigma = 0.2$, the dominant frequency of the slave oscillator Ω_2 is entrained by the master oscillator [Fig. 6(d)], resulting in phase synchronization [Fig. 6(b)]. One can see in Fig. 6(f) that
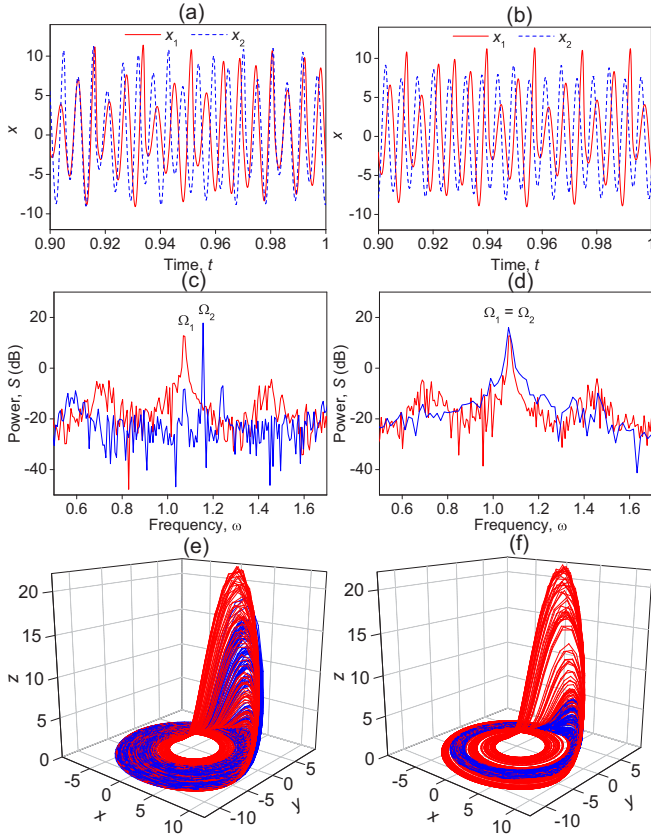
FIG. 6. Numerical [(a) and (b)] time series, [(c) and (d)] power spectra, and [(e) and (f)] chaotic attractors of two [(a), (c), and (e)] uncoupled and [(b), (d), and (f)] coupled Rössler oscillators [Eq. (3)]. Coherence enhancement of the slave oscillator observed for frequency mismatch $\Delta = 0.1$ and coupling $\sigma = 0.2$ when its dominant frequency is entrained by the master oscillator.
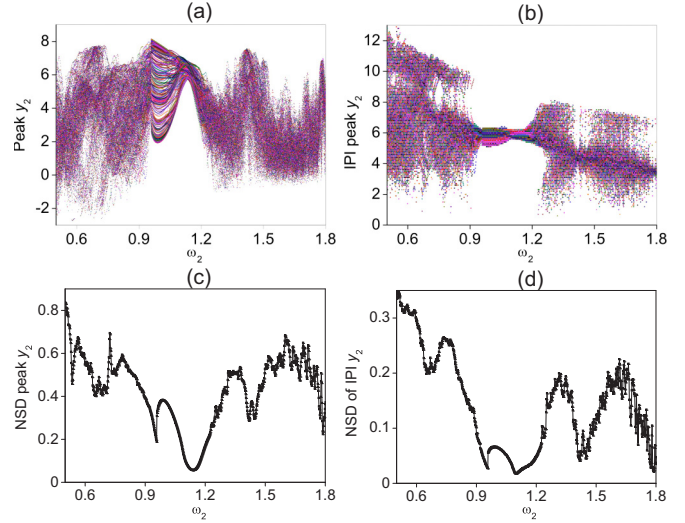

FIG. 7. Numerical (a) peak value of y_2, (b) IPI, (c) NSD of peak y_2, and (d) NSD of IPI as a function of natural frequency of slave oscillator ω_2 for $\sigma = 0.2$ and $\omega_1 = 1$.

and lag synchronization of nonidentical chaotic oscillators:

$$S_{ij}^2(\tau) = \frac{\langle [x_j(t) - x_i(t + \tau)]^2 \rangle}{\sqrt{\langle x_j(t)^2 \rangle \langle x_i(t)^2 \rangle}}, \qquad (4)$$

where τ is the time shift between the state vectors of the interacting systems. The lower the minimum of the similarity function $\delta = \min_\tau S(\tau)$, the better the synchronization. Figure 9 shows how the minimum similarity between two coupled oscillators, δ_{12}, depends on both the natural frequency

the chaotic attractor of the slave oscillator shrinks, meaning that its dynamics becomes more regular.

Figure 7 demonstrates coherence resonance in the slave oscillator with respect to its natural frequency, while the natural frequency of the master oscillator remains fixed to $\omega_1 = 1$.

The bifurcation diagrams of the peak value of the variable y_2 [Fig. 7(a)] and the interpeak interval (IPI) [Fig. 7(b)] display strong resonant suppression of the amplitude variation at $\omega_2 = 1.14$. The coherence resonances in amplitude and time are clearly seen in Figs. 7(c) and 7(d), respectively.

In Fig. 8 we plot NSD of peak y_2 [Fig. 8(a)] and IPI [Fig. 8(b)] in the space of two control parameters, the natural frequency ω_2 of the slave oscillator and the coupling strength σ. These diagrams have a structure of Arnold tongues centered at $\omega_2 = 1$. Within these tongues, the dominant frequency of the slave oscillator is entrained by the master oscillator, so the oscillators are in phase synchronization. The dark blue bands inside these tongues indicate the region of higher coherence.

The interesting question may arise of whether the coherence resonance is related to synchronization. To measure synchronization we use similarity function S_{ij} between the oscillators i and j introduced by Rosenblum et al. [51] to describe phase

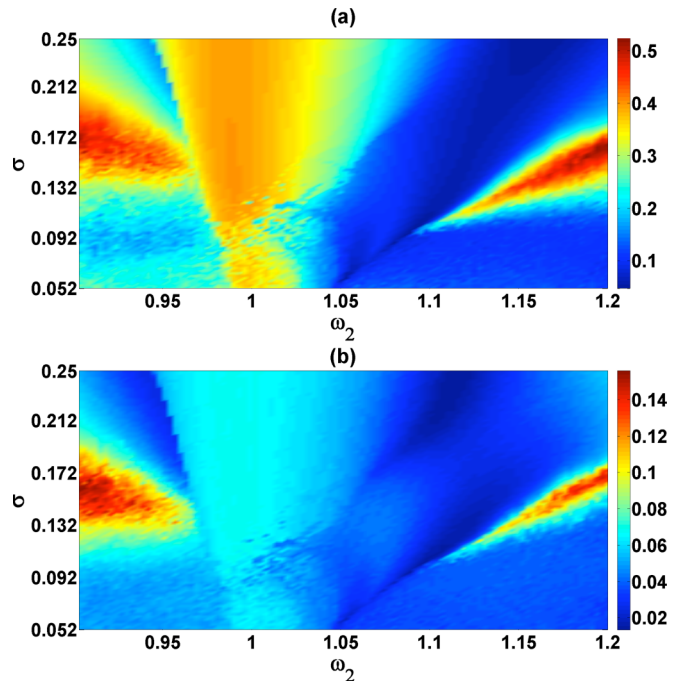

FIG. 8. Normalized standard deviations of (a) peak y_2 and (b) interpeak intervals in (ω_2, σ)-parameter space. The violet (dark) regions are associated with increasing coherence.
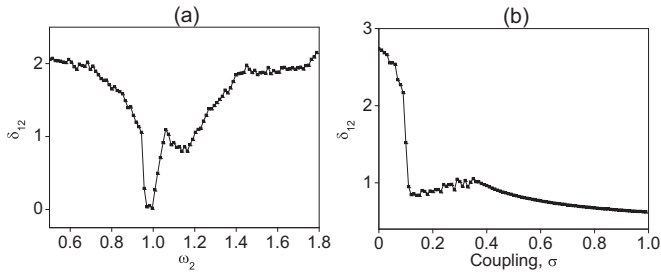
FIG. 9. Minimum similarity as a function of (a) natural frequency of slave oscillator ω_2 for $\sigma = 0.2$ and (b) coupling σ for $\omega_2 = 1.1$.

of the slave oscillator ω_2 [Fig. 9(a)] and the coupling strength σ [Fig. 9(b)]. The slump of the dependence in Fig. 9(a) close to $\omega_2 = 1$ results from phase synchronization when the natural frequency of the slave oscillator ω_2 approaches the natural frequency of the master oscillator $\omega_1 = 1$. When the oscillators' natural frequencies exactly match ($\omega_2 = \omega_1 = 1$), complete synchronization is observed ($\delta_{12} = 0$) because in this case we deal with identical systems. Another, local, minimum at $\omega_2 = 1.14$ coincides with the deterministic coherence resonance in Fig. 7. This means that enhanced coherence is accompanied by improving phase synchronization. Note that changes in the similarity function associated with coherence resonance are only present in the frequency dependence in Fig. 9(a) but not in the dependence on the coupling strength. Indeed, as one can see from Fig. 8, the maximal coherence occurs for $\sigma = 0.2$ without qualitative changes for this value in Fig. 9(b). Evidently, synchronization measures cannot be used to characterize coherence because the latter occurs in one (slave) oscillator only, while synchronization refers to a relative behavior between two oscillatory systems.

Next, we analyze the Lyapunov exponent spectrum in order to demonstrate how the control parameters affect the system stability. Since the dynamics of the master oscillator does not depend on the control parameters, the stability of the whole system is determined by the dynamics of the slave oscillator only. All six Lyapunov exponents λ_{1-6} are plotted in Fig. 10 in the (ω_2, σ)-parameter space.

Since the master oscillator is chaotic, the first largest Lyapunov exponent λ_1 [Fig. 10(a)] is always positive for all control parameters. Depending on the control parameters, the second exponent λ_2 [Fig. 10(b)] is either positive or zero. The most important information about the system stability can be extracted from the divergence or convergence of the phase-space trajectory towards the directions of the slave oscillator variables, i.e., the third and fourth Lyapunov exponents, λ_3 and λ_4. One can see from Figs. 10(c) and 10(d) that these exponents take negative values and reach minima in the dark (blue) region in the parameter range $1.1 < \omega_2 < 1.15$ and $\sigma > 0.13$, corresponding to the best coherence of the slave oscillator. Lower Lyapunov exponents, i.e., higher stability of the system, are associated with coherence enhancement. However, in the region of complete synchronization when the oscillators are identical ($\omega_2 = \omega_1 = 1$), these exponents are close to zero. By comparing the NSD diagrams in Fig. 9 with the Lyapunov exponents in Fig. 10 we can see their strong
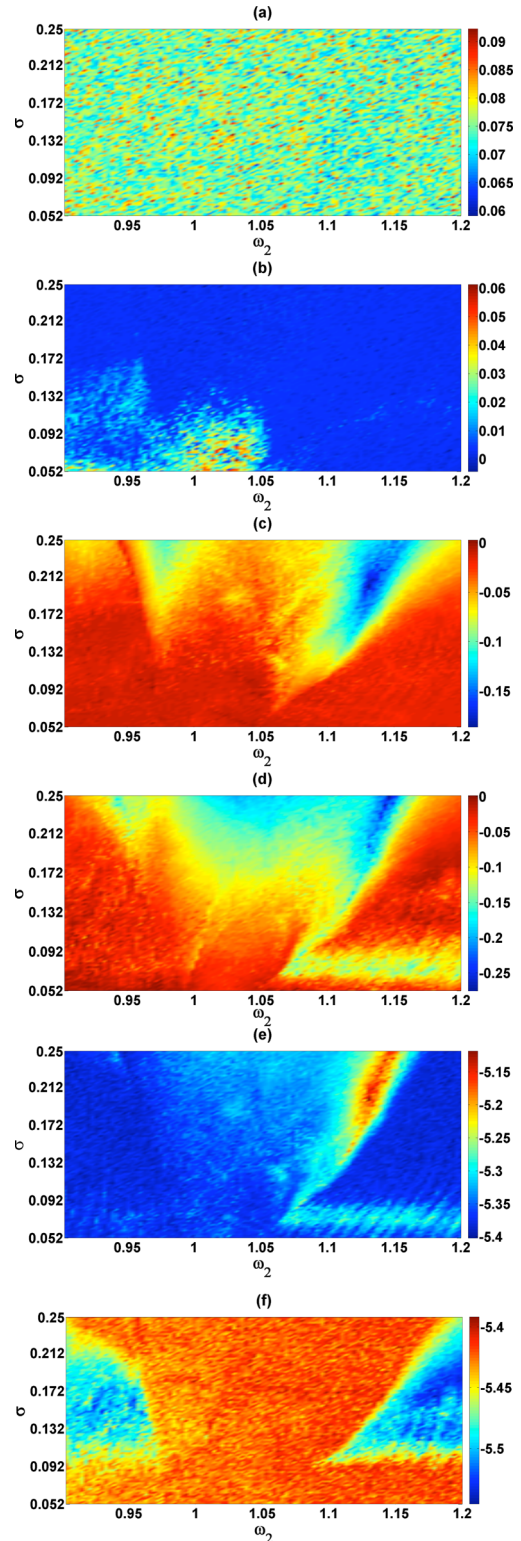

FIG. 10. Lyapunov exponents [(a)–(f)] λ_{1-6} of two coupled oscillators in (ω_2, σ)-parameter space. Deterministic coherence resonance is associated with negative λ_3 and λ_4 in the region of the central blue (dark) spots in (c) and (d).

correlation in the region of the coherence resonance where the minimum NSD matches the minima of the third and fourth Lyapunov exponents. The fifth and sixth Lyapunov exponents, λ_5 and λ_6, do not yield additional information because they are
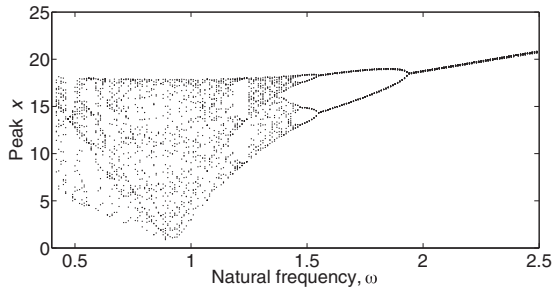
FIG. 11. Numerical bifurcation diagram of peak x with respect to natural frequency of the uncoupled Rössler oscillator.

always negative in the explored parameter range [Figs. 10(e) and 10(f)].

B. Three coupled oscillators

For numerical simulations of the three Rössler oscillators unidirectionally coupled in a ring we choose the parameters $a = 0.165$, $b = 0.2$, and $c = 10$ because for these parameters the uncoupled oscillator exhibits a chaotic regime in a wide range of the natural frequency, as shown in the bifurcation diagram in Fig. 11. This allows us to vary significantly the distance between the oscillators (frequency mismatch) as long as they remain chaotic.

For simplicity, we consider a symmetric case where the distances between the oscillators 1 and 2 and the oscillators 2 and 3 are the same, i.e., $\Delta_{21} = \Delta_{32} = \Delta_{13}/2 = \Delta$. To study the influence of the detuning Δ on the coherence, we fix the natural frequency of the oscillator 2 to $\omega_2 = 0.9$ and use Δ as a control parameter. Figure 12 shows the time series, phase portraits, and power spectra of the x variable of the uncoupled [Figs. 12(a) and 12(c)] and coupled oscillators with the coupling strength $\sigma = 0.2$ [Figs. 12(c) and 12(d)].

Being uncoupled, the oscillators are chaotic with different dominant frequencies in their power spectra [Fig. 12(c)]. As
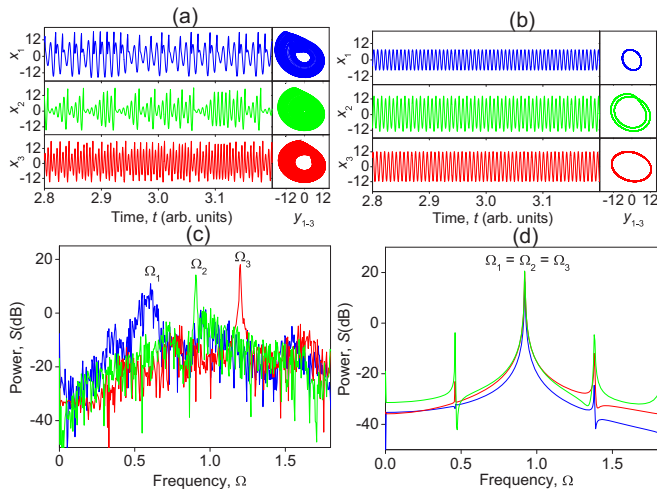

FIG. 12. Numerical [(a) and (b)] time series, phase portraits, and [(c) and (d)] power spectra of three [(a) and (c)] uncoupled and [(b) and (d)] coupled Rössler oscillators for $\sigma = 0.33$ and $\Delta = 0.2$. The coupled oscillators behave periodically.
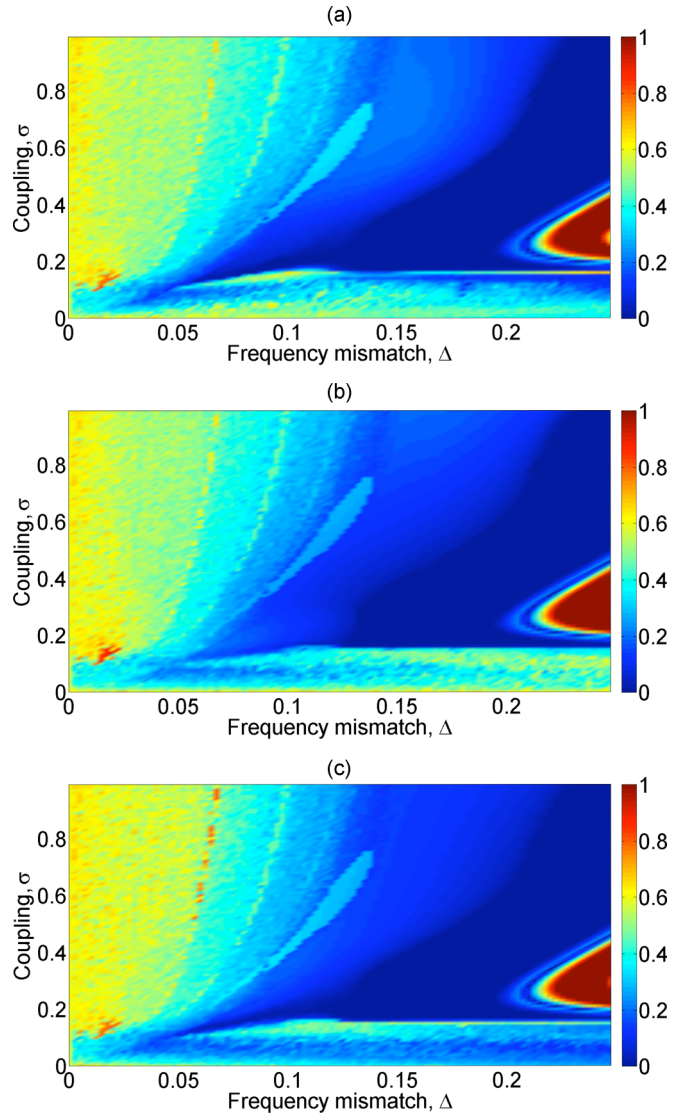

FIG. 13. NSD of peak (a) x_1, (b) x_2, and (c) x_3 in (Δ,σ)-parameter space.

the coupling strength σ is increased, the oscillators' phases synchronize, resulting in the same dominant frequency in their power spectra [Fig. 12(d)]. When σ is further increased, they oscillate in a period-2 regime [Fig. 12(b)]. These results are in good agreement with the experiment.

Figure 13 shows NSD of the peak value of the variable x for every oscillator as a function of both frequency mismatch (distance) Δ and coupling strength σ. While for small distances, all oscillators are incoherent (chaotic) [left-hand (green) tongues], they become highly coherent for intermediate distances and coupling [right-hand (dark blue) tongues]. Therefore, there exists a preferential coupling for which the coherence is maximized. High NSD for $\Delta > 0.2$ and $0.2 < \sigma < 0.4$ does not mean low coherence; this occurs because for these parameters the oscillators are involved in a period-doubling regime where the difference between amplitudes of subsequent peaks is large.

The resonance behavior with respect to both the coupling strength and the distance is clearly seen in Fig. 14, where
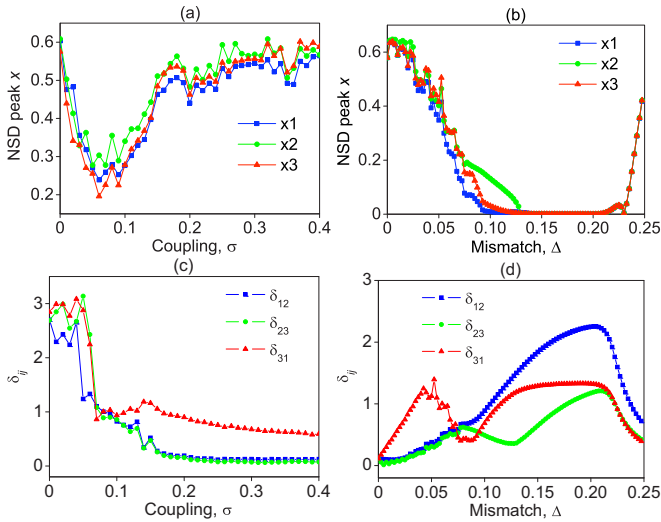
FIG. 15. Largest Lyapunov exponent of three ring-coupled oscillators in (Δ, σ)-parameter space. The blue dark tongue indicates the region of coherence resonance and periodicity for large Δ and intermediate σ.

FIG. 14. [(a) and (b)] NSD of peak x versus (a) coupling for $\Delta = 0.03$ and (b) mismatch for $\sigma = 0.2$. The minima of NSD indicate coherence resonance. [(c) and (d)] Minimum similarity versus (c) coupling for $\Delta = 0.03$ and (d) mismatch for $\sigma = 0.2$. The maxima δ_{ij} at $\Delta \approx 0.2$ indicate partial desynchronization.

we present one-dimensional plots of NSDs for fixed $\Delta = 0.03$ [Fig. 14(a)] and fixed $\sigma = 0.2$ [Fig. 14(b)]. In Fig. 14(a), NSDs of the peak x of all oscillators take minimal values at $\sigma \approx 0.08$ displaying the coherence resonance behavior. In Fig. 14(b), the coherence enhancement is observed in a wide range of distances $(0.1 < \Delta < 0.23)$.

In the previous section we have shown that in the case of two coupled oscillators the coherence resonance was accompanied by improving phase synchronization. Now we are interested in how the enhancing coherence affects synchronization in the case of three ring-coupled oscillators. In Fig. 14(c) we plot the minimum similarity δ_{ij} for each pair of the coupled oscillators as a function of the coupling strength for the same detuning $\Delta = 0.03$ as in Fig. 14(a). When the coupling is small $(\sigma < 0.05)$, δ_{ij} is very large, meaning that the oscillators are asynchronous. A sudden slump in δ_{ij} near $\sigma = 0.05$ indicates the onset of phase synchronization. By comparing Fig. 14(a) with Fig. 14(c) one can see that the coherence resonance occurs near the onset of phase synchronization. As the coupling increases, δ_{ij} slowly decreases, meaning there is improved phase synchronization. The evident situation, that synchronization of the oscillators 1 and 3 with the largest frequency mismatch is worse than the synchronization of other pairs of oscillators with smaller mismatch, is illustrated in Fig. 14(c).

The effect of the frequency mismatch on synchronization is demonstrated in Fig. 14(d). When $\Delta = 0$ the oscillators are identical and therefore completely synchronized. As Δ is increased, δ_{ij} also increases, leading to desynchronization. For small Δ the minimum similarity of the oscillators 1 and 3 (δ_{31}) with the largest frequency mismatch is higher than δ_{ij} of other, closer located oscillators. The maxima of δ_{ij} at $\Delta \approx 0.2$ mean partial desynchronization due to coherence enhancement, i.e., the oscillators are less similar in spite of higher coherence.
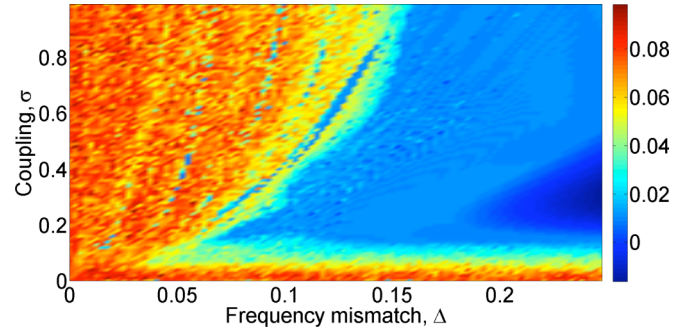
It is important to check whether the coupled system does become stable in a certain region of the coupling strength and frequency mismatch. For this purpose we analyze the system stability through Lyapunov exponents. In Fig. 15 we plot the largest Lyapunov exponent in the parameter space of distance Δ and coupling σ.

When the oscillators' frequencies are very close to each other, they are chaotic for any coupling strength, whereas for larger distances their dynamics become more regular. The comparison of Figs. 15 and 13 shows that the coherence enhancement is associated with increasing system stability in the dark blue tongue. Indeed, for relatively large distances $(\Delta > 0.1)$ and intermediate coupling $(0.1 < \sigma > 0.4)$ the largest Lyapunov exponent takes negative values; in this parameter region a period-2 orbit is stabilized.

IV. CONCLUSION

In this paper we have presented the experimental evidence of the appearance of order in a chaotic system under the influence of a chaotic signal generated by another similar system. Such coherence enhancement has been demonstrated in two and three unidirectionally coupled Rössler oscillators with small mismatch between their natural frequencies. The enhanced coherence has a resonant character with respect to the coupling strength and frequency mismatch.

To characterize this deterministic coherence resonance we have used the normalized standard deviations of the peak amplitude and interpeak interval. In the case of two coupled oscillators the coherence resonance is accompanied by improved phase synchronization, while in the ring of three oscillators it is associated with partial desynchronization. In the latter case the stabilization of a periodic orbit has been observed. The results of the numerical simulations are in good agreement with the experimental results.

The analysis of the Lyapunov exponent spectra has shown that in two coupled oscillators, the coherence enhancement is associated with negative third and fourth Lyapunov exponents, while in the ring of three oscillators, all Lyapunov exponents

take negative values in a certain range of the frequency mismatch and coupling strength. The last phenomenon is the manifestation of self-stabilization of coupled chaotic systems due to their interaction.

[1] I. Prigogine and I. Stengers, *Order Out of Chaos* (Bantam Books, New York, 1984).

[2] A. L. Fradkov and A. Yu. Pogromsky, *Introduction to Control of Oscillations and Chaos* (World Scientific, Singapore, 1998).

[3] E. Schöll and H. G. Schuster, *Handbook of Chaos Control* (Wiley-VCH, Weinheim, 2007).

[4] E. Ott, C. Grebogi, and J. A. Yorke, Phys. Rev. Lett. **64**, 1196 (1990).

[5] K. Pyragas, Phys. Lett. A **170**, 421 (1992).

[6] R. Lima and M. Pettini, Phys. Rev. A **41**, 726 (1990).

[7] Y. Braiman and I. Goldhirsch, Phys. Rev. Lett. **66**, 2545 (1991).

[8] R. Meucci, W. Gadomski, M. Ciofini, and F. T. Arecchi, Phys. Rev. E **49**, R2528(R) (1994).

[9] A. N. Pisarchik, V. N. Chizhevsky, R. Corbalán, and R. Vilaseca, Phys. Rev. E **55**, 2455 (1997).

[10] A. N. Pisarchik, B. F. Kuntsevich, and R. Corbalán, Phys. Rev. E **57**, 4046 (1998).

[11] A. S. Pikovsky and J. Kurths, Phys. Rev. Lett. **78**, 775 (1997).

[12] Hu Gang, T. Ditzinger, C. Z. Ning, and H. Haken, Phys. Rev. Lett. **71**, 807 (1993).

[13] A. Neiman, P. I. Saparin, and L. Stone, Phys. Rev. E **56**, 270 (1997).

[14] D. E. Postnov, S. K. Han, T. G. Yim, and O. V. Sosnovtseva, Phys. Rev. E **59**, R3791(R) (1999).

[15] G. Giacomelli, M. Giudici, S. Balle, and J. R. Tredicce, Phys. Rev. Lett. **84**, 3298 (2000).

[16] B. Lindner, J. García-Ojalvo, A. Neiman, and L. Schimansky-Geier, Phys. Rep. **392**, 321 (2004).

[17] L. S. Tsimring and A. Pikovsky, Phys. Rev. Lett. **87**, 250602 (2001).

[18] K. Panajotov, M. Sciamanna, A. Tabaka, P. Megret, M. Blondel, G. Giacomelli, F. Marin, H. Thienpont, and I. Veretennicoff, Phys. Rev. A **69**, 011801(R) (2004).

[19] M. Arizaleta Arteaga, M. Valencia, M. Sciamanna, H. Thienpont, M. López-Amo, and K. Panajotov, Phys. Rev. Lett. **99**, 023903 (2007).

[20] M. Franaszek and E. Simiu, Phys. Rev. E **54**, 1298 (1996).

[21] A. N. Pisarchik and R. Corbalán, Phys. Rev. E **58**, R2697 (1998).

[22] K. Arai, K. Yoshimura, and S. Mizutani, Phys. Rev. E **65**, 015202 (2001).

[23] J. F. Martinez Avila, H. L. D. de S. Cavalcante, and J. R. Rios Leite, Phys. Rev. Lett. **93**, 144101 (2004).

[24] Y. Hong and K. A. Shore, IEEE J. Quantum Electron. **41**, 1054 (2005).

[25] A. Karsaklian Dal Bosco, D. Wolfersbergerand, and M. Sciamanna, Eur. Phys. Lett. **101**, 24001 (2013).

[26] J. Buryk, A. Krawiecki, and T. Buchner, Chaotic Modeling and Simulation **2**, 363 (2012).

[27] S. Camazine, J.-L. Deneubourg, N. R. Franks, J. Sneyd, G. Theraulaz, and E. Bonabeau, *Self-Organization in Biological Systems* (Princeton University Press, NJ, 2001).

[28] S. Strogatz, *Sync: The Emerging Science of Spontaneous Order* (Hyperion, New York, 2003).

[29] K. Bar-Eli, Physica D **14**, 242 (1985).

[30] P. C. Matthews and S. H. Strogatz, Phys. Rev. Lett. **65**, 1701 (1990).

[31] J. Bragard, G. Vidal, H. Mancini, C. Mendoza, and S. Boccaletti, Chaos **17**, 043107 (2007).

[32] A. N. Pisarchik and R. Jaimes-Reátegui, Phys. Rev. E **92**, 050901(R) (2015).

[33] A. Pikovsky, M. Rosenblum, and J. Kurths, *Synchronization: A Universal Concept in Nonlinear Science* (Cambridge University Press, New York, 2001).

[34] A. S. Pikovsky, M. G. Rosenblum, and J. Kurths, Europhys. Lett. **34**, 165 (1996).

[35] M. G. Rosenblum, A. S. Pikovsky, and J. Kurths, Phys. Rev. Lett. **76**, 1804 (1996).

[36] S. Boccaletti, J. Kurths, G. Osipov, D. L. Valladares, and C. S. Zhou, Phys. Rep. **366**, 1 (2002).

[37] V. S. Anischenko and T. E. Vadivasova, Radiotekh. Elektron. (Moscow) **47**, 133 (2002) [J. Commun. Technol. Electron. **47**, 117 (2002)].

[38] S. Boccaletti, E. Allaria, R. Meucci, and F. T. Arecchi, Phys. Rev. Lett. **89**, 194101 (2002).

[39] U. Parlitz, L. Junge, W. Lauterborn, and L. Kocarev, Phys. Rev. E **54**, 2115 (1996).

[40] T. L. Carroll, Phys. Rev. E **64**, 015201 (2001).

[41] P. K. Roy, S. Chakraborty, and S. K. Dana, Chaos **13**, 342 (2003).

[42] C. Schäfer, M. G. Rosenblum, J. Kurths, and H.-H. Abel, Nature (London) **392**, 239 (1998).

[43] V. Makarenko and R. Llinás, Proc. Natl. Acad. Sci. U.S.A. **95**, 15747 (1998).

[44] P. Tass, M. G. Rosenblum, J. Weule, J. Kurths, A. S. Pikovsky, J. Volkmann, A. Schnitzler, and H.-J. Freund, Phys. Rev. Lett. **81**, 3291 (1998).

[45] J. Bhattacharya and H. Petsche, Phys. Rev. E **64**, 012902 (2001).

[46] B. Blasius, A. Huppert, and L. Stone, Nature (London) **399**, 354 (1999).

[47] B. Blasius and L. Stone, Int. J. Bifurcation Chaos Appl. Sci. Eng. **10**, 2361 (2000).

[48] T. Pyragiené and K. Pyragas, Nonlinear Dyn. **74**, 297 (2013).

[49] O. E. Rössler, Phys. Lett. A **57**, 397 (1976).

[50] See Supplemental Materials at http://link.aps.org/supplemental/10.1103/PhysRevE.94.012218 Video demonstrated the emergence of coherence resonance in two unidirectionally coupled chaotic electronic circuits.

[51] M. G. Rosenblum, A. S. Pikovsky, and J. Kurths, Phys. Rev. Lett. **78**, 4193 (1997).